

**HHS PUBLIC ACCESS**

Author manuscript

Nat Med. Author manuscript; available in PMC 2011 February 01.

Published in final edited form as:

Nat Med. 2010 August ; 16(8): 872–879. doi:10.1038/nm.2181.

**CIB1 is a Regulator of Pathological Cardiac Hypertrophy****Joerg Heineke<sup>1,2,\*</sup>, Mannix Auger-Messier<sup>1,\*</sup>, Robert N. Correll<sup>1</sup>, Jian Xu<sup>1</sup>, Matthew J. Benard<sup>1</sup>, Weiping Yuan<sup>3</sup>, Helmut Drexler<sup>2</sup>, Leslie V. Parise<sup>3</sup>, and Jeffery D. Molkentin<sup>1</sup>**<sup>1</sup> Howard Hughes Medical Institute, Department of Pediatrics, University of Cincinnati, Cincinnati Children's Hospital Medical Center, 240 Albert Sabin Way, Cincinnati, OH 45229, USA<sup>2</sup> Medizinische Hochschule Hannover, Klinik für Kardiologie und Angiologie, Cluster of Excellence Rebirth, Carl-Neuberg-Str.1, 30625 Hannover, Germany<sup>3</sup> Department of Biochemistry and Biophysics, School of Medicine, University of North Carolina at Chapel Hill, CB 7260, Chapel Hill, NC 27599, USA**Abstract**

Hypertrophic heart disease is a leading health problem facing the Western world. Here we identified the small EF-hand domain-containing protein CIB1 (Ca<sup>2+</sup> and integrin binding protein 1) in a screen for novel regulators of cardiomyocyte hypertrophy. Yeast two-hybrid screening for CIB1 interacting partners identified a related EF-hand domain-containing protein calcineurin B, the regulatory subunit of the pro-hypertrophic protein phosphatase calcineurin. CIB1 largely localizes to the sarcolemma in mouse and human myocardium, where it anchors calcineurin to control its activation in coordination with the L-type Ca<sup>2+</sup> channel. CIB1 protein levels and membrane association were enhanced in cardiac pathological hypertrophy, but not in physiological hypertrophy. Consistent with these observations, mice lacking *Cib1* show a dramatic reduction in myocardial hypertrophy, fibrosis, cardiac dysfunction, and calcineurin-NFAT activity following pressure overload, while the degree of physiologic hypertrophy after swimming was not altered. Transgenic mice with inducible and cardiac-specific overexpression of CIB1 showed enhanced cardiac hypertrophy in response to pressure overload or calcineurin signaling. Moreover, mice lacking the *Ppp3cb* gene showed no enhancement in cardiac hypertrophy associated with CIB1 overexpression. Thus, CIB1 functions as a novel regulator of cardiac hypertrophy through its ability to regulate calcineurin sarcolemmal association and activation.

---

Heart failure is a serious disease with an 8-year mortality rate between 70 and 80%<sup>1</sup>. One of the major risk factors for developing heart failure is pre-existing cardiac hypertrophy that

---

Users may view, print, copy, download and text and data-mine the content in such documents, for the purposes of academic research, subject always to the full Conditions of use: [http://www.nature.com/authors/editorial\\_policies/license.html#terms](http://www.nature.com/authors/editorial_policies/license.html#terms)

Correspondence should be addressed to J.D.M. ([jeff.molkentin@cchmc.org](mailto:jeff.molkentin@cchmc.org)), or J.H. ([Heineke.Joerg@mh-hannover.de](mailto:Heineke.Joerg@mh-hannover.de)).

\*These authors contributed equally

**Competing Interests Statement**

The authors declare no financial or competing interests related to this work.

**Author Contributions**J.H. performed and planned most of the experimentation with technical help from J.X., M. A.-M., R.N.C., and M.J.B. W.Y., and L.V.P. provided *Cib1*<sup>-/-</sup> mice and recombinant CIB1 protein. J.D.M. planned and supervised all experimentation. H.D. provided experimental support and ideas for the project. J.H. and J.D.M. wrote the paper.

results from pathologic stimuli such as long-standing hypertension or myocardial infarction<sup>2</sup>. The intracellular signaling pathways involved in the regulation of myocardial growth have been studied in great detail over the past decade<sup>3</sup>. One major pro-hypertrophic signaling pathway involves the serine-threonine protein phosphatase calcineurin, which is directly activated by Ca<sup>2+</sup>-calmodulin binding when intracellular Ca<sup>2+</sup> levels rise. Activated calcineurin directly binds and dephosphorylates a family of transcription factors known as nuclear factor of activated T cells (NFAT), causing nuclear translocation and activation of hypertrophic gene expression<sup>4</sup>. Calcineurin is a heterodimer of a 58–64 kDa catalytic subunit, calcineurin A (CnA), and a 19 kDa regulatory subunit, calcineurin B (CnB)<sup>4</sup>. Calcineurin can localize to the plasma membrane of cardiac myocytes (sarcolemma) and membrane invaginations called T-tubules, which overlay the cytoskeletal Z-discs<sup>5–8</sup>. Calcineurin can also associate with membrane phospholipids through its regulatory subunit CnB<sup>9</sup>. However, it remains uncertain how calcineurin is regulated by Ca<sup>2+</sup> in a contracting cell such as a cardiac myocyte given the dynamic range of Ca<sup>2+</sup> fluctuations that occur throughout the cytosol to mediate contraction. Partial localization to defined membrane microdomains might be one possibility. Indeed, calcineurin was recently shown to directly bind the L-type Ca<sup>2+</sup> channel within the sarcolemma, potentially receiving a direct source of Ca<sup>2+</sup> for activation<sup>10</sup>.

In this study we identified CIB1 (also called calmyrin) as a novel regulator of calcineurin-NFAT signaling and cardiac hypertrophy. CIB1 is widely expressed in various human and mouse tissues with particularly high expression in the heart<sup>11–13</sup>. CIB1 is a 22 kDa protein containing 4 EF-hand domains, although only the third and fourth C-terminal EF-hands functionally bind Ca<sup>2+</sup> at physiologic concentrations<sup>14</sup>. CIB1 can be myristoylated at its N-terminus to mediate plasma-membrane localization in multiple cell types<sup>13–15</sup>. CIB1 can also interact with multiple signaling proteins that reside near the plasma-membrane, such as integrin  $\alpha_{IIb}\beta_3$ , focal adhesion kinase (FAK), the small GTPase Rac3, p21-activated kinase (PAK1), and sphingosine kinase 1<sup>15–19</sup>. Functionally, while *Cib1*<sup>-/-</sup> mice are viable, they show a defect in spermatogenesis leading to sterility in males, as well as a defect in angiogenesis following ischemia<sup>20,21</sup>.

## RESULTS

### Characterization of myocardial CIB1 expression

In an effort to identify novel regulators of cardiomyocyte growth, we performed mRNA array screens for genes that were induced by GATA4 overexpression in cultured neonatal rat cardiomyocytes, which identified CIB1. Western and Northern blotting confirmed that hypertrophy induced by AdGATA4 (GATA4 recombinant adenovirus) infection strongly induced CIB1 expression in neonatal cardiomyocytes compared with Ad $\beta$ gal control infection (Fig. 1a, and Supplemental Fig. 1a). Analysis of CIB1 heart expression in vivo by Western blotting and immunohistochemistry revealed high levels at embryonic (E) day 16, at birth, and 1 week after birth, with progressive reductions in expression with aging (Fig. 1b,c, and Supplemental Fig. 1b). Interestingly, CIB1's localization within cardiac myocytes shifts from a more diffuse cytoplasmatic position before birth to the sarcolemma in the adult heart (Fig. 1c).

Given the induction of CIB1 by GATA4 in neonatal cardiomyocytes, we hypothesized that it might also be induced in the adult heart by pro-hypertrophic stimuli. Indeed, myocardial CIB1 mRNA and protein levels were upregulated by 2-fold after 2 weeks of pressure overload stimulation by transverse aortic constriction (TAC) compared to sham operated controls (Fig. 1d,e, and Supplemental Fig. 1c). Immunohistochemistry revealed enhanced membrane localization of the protein after 2 weeks of pressure overload, but no induction or increased membrane localization in hearts from mice with physiologic hypertrophy due to swimming (Fig. 1e,f). CIB1 was also detected at the sarcolemma in control human heart histological sections, and consistent with our observations in hypertrophied mouse hearts, more CIB1 was observed at the sarcolemma in hypertrophied samples (Fig. 1g).

### CIB1 deficiency inhibits pathological cardiac growth

The increase in CIB1 protein expression and membrane localization during hypertrophic growth suggested a potential functional role in this process. To directly address this hypothesis, we subjected heterozygous and homozygous *Cib1* gene-targeted mice to 2 weeks of TAC, which showed reduced or absent CIB1 protein in the heart, respectively (Fig. 2a). Remarkably, myocardial growth was reduced in a dose-dependent manner in *Cib1* heterozygous and null mice compared with strain-matched wildtype (WT) control mice (Fig. 2b). Exposure to pressure overload was similar, as the pressure gradient across the aortic constriction was not statistically different between the 3 TAC groups (Supplemental Fig. 2a). Evaluation of cardiomyocyte cross-sectional areas in histological sections from WT and *Cib1*<sup>-/-</sup> hearts after TAC revealed a similar reduction in cellular growth (Fig. 2c). Consistent with these data, *Cib1*<sup>-/-</sup> mice showed less mRNA induction of the hypertrophic marker gene atrial natriuretic factor (ANF) and  $\beta$ -myosin heavy chain (MHC) after 2 weeks of TAC compared with WT controls (Fig. 2d, and Supplemental Fig. 2b). Finally, we assessed capillary density because CIB1 was previously shown to be necessary for ischemic angiogenesis outside the heart<sup>21</sup>. Capillary density normalized to myocyte content was not different between *Cib1*<sup>-/-</sup> and WT hearts after a sham and TAC operation (Supplemental Fig 2c,e). However, when not normalized to myocyte content, *Cib1*<sup>-/-</sup> hearts actually showed more capillaries per total histological section after TAC, which could be another protective mechanism in these hearts (Supplemental Fig 2d,e). This later result can be explained because TAC is known to induce angiogenesis in the heart, and in the absence of hypertrophy the relative density of capillaries becomes increased relative to myocyte area.

To determine the impact of CIB1 deficiency on heart failure predisposition, we subjected WT and *Cib1*<sup>-/-</sup> mice to 6 weeks of pressure overload and determined cardiac function every week by echocardiography. While the initial pressure gradient imposed by TAC was not different between WT and *Cib1*<sup>-/-</sup> mice (Supplemental Fig. 3a), WT mice showed significantly greater reductions in fractional shortening (FS) compared with *Cib1*<sup>-/-</sup> mice 3 to 6 weeks post TAC (Fig. 2e, P<0.05). Histological analysis with Masson's trichrome staining and subsequent quantification of the fibrotic area (blue staining) by MetaMorph<sup>®</sup> software revealed significantly more fibrosis in the hearts of WT mice compared to *Cib1*<sup>-/-</sup> mice after 6 weeks of TAC (Fig. 2f,g, P<0.05). This result was corroborated by measuring hydroxyproline content in the heart as an indicator of collagen (Supplemental Fig. 3b). Taken together, these results indicate that CIB1 is involved in regulating the pathologic

hypertrophic response of the myocardium to pressure overload stimulation, as well as secondary decompensation. In support of CIB1's role in preferentially regulating pathological cardiac hypertrophy, loss of this protein did not attenuate physiological cardiac hypertrophy in response to swimming exercise. (Fig. 2h).

Because CIB1 was induced in pathological cardiac hypertrophy, it was of interest to determine if it could also regulate the hypertrophic response in cultured neonatal cardiac myocytes. To this end, endogenous CIB1 expression was reduced with a specific siRNA (Supplemental Fig. 3c). CIB1 siRNA transfection significantly reduced the increase in cell growth and hypertrophic marker gene expression (ANF and b-type natriuretic peptide [BNP]) induced by the pro-hypertrophic  $\alpha$ 1-adrenergic agonist phenylephrine (PE) (Supplemental Fig. 3d–f,  $P < 0.05$ ).

### CIB1 interacts with CnB

That *Cib1*<sup>-/-</sup> mice were partially protected from pathologic hypertrophy suggested a function in regulating intracellular signaling, especially since CIB1 has already been shown to interact with select signaling effectors<sup>15–19</sup>. We first investigated the activation status of a wide array of signaling pathways in response to CIB1 overexpression or deletion. However, no alterations were observed in the activation of extracellular signal-regulated kinases (ERK1/2), p38 mitogen-activated protein kinase (MAPK), c-Jun N-terminal kinase (JNK), Akt, glycogen synthase kinase 3 $\beta$  (GSK3 $\beta$ ) or nuclear factor  $\kappa$ B (Supplemental Fig. 4). Given these negative results, we turned to a yeast two-hybrid assay to identify CIB1 interacting proteins and determine how it might be signaling in cardiac myocytes. Using this approach we obtained three independent cDNA preys containing CnB, including both the short and long isoform. Re-transformation of the CIB1 bait and CnB preys in yeast confirmed an interaction that was similar in intensity to a positive control consisting of CnA bait with CnB prey (Fig. 3a). To show that the interaction of these two proteins occurs in cardiac myocytes, we performed immunoprecipitation of CnB or CnA after overexpression of each, which pulled down CIB1 in both cases (Fig. 3b,c). Moreover, immunoprecipitation of endogenous CIB1 pulled down endogenous CnB from WT hearts, without overexpression (Fig. 3d). Since the short isoform of CnB is by far the most abundant isoform in the heart (Supplemental Fig. 5), we subsequently focused our attention on the interaction of CnB<sub>short</sub> with CIB1. We incubated in vitro synthesized and <sup>35</sup>S-methionine-labeled CnB with GST-CIB1 full-length and deletion proteins, as well as with GST alone. The data show that GST alone, GST-CIB1 1–55 (amino acids), 1–82 and 1–108 did not interact with CnB, while GST-CIB1-full length and GST-CIB1 1–132 did interact (Fig. 3e). Therefore, the region corresponding to the functional C-terminal EF-hand domains of CIB1 is responsible for the interaction with CnB.

### CIB1 mediates CnB association with the sarcolemma

CIB1 is a myristoylated protein suggesting that CIB1 might regulate calcineurin membrane localization and activity. To test this hypothesis, we performed CnB immunostaining in frozen sections from WT and *Cib1*<sup>-/-</sup> hearts after sham and TAC surgery. Compared with membrane localization in sham hearts, slightly enhanced levels of CnB localization/staining was observed in hearts of WT mice subjected to TAC, although CnB was not detected at the

membrane in *Cib1*<sup>-/-</sup> hearts at baseline or after TAC (Fig. 4a). To exclude the possibility that protein abundance of CnB or CnA was changed in the *Cib1*<sup>-/-</sup> hearts, CnA or CnB protein levels were examined and determined not to significantly differ between WT or *Cib1*<sup>-/-</sup> hearts after TAC stimulation, although there was a trend toward an increase in CnA after TAC in WT hearts (Fig. 4b, P<0.05). However, in agreement with the immunohistochemical results, CnB and CnA protein could only be detected in the plasma-membrane fraction of WT TAC hearts, but not *Cib1*<sup>-/-</sup> hearts (Fig. 4c). The cytosolic fraction, which holds markedly more CnB and CnA compared to the plasma-membrane, contained equal amounts of CnB in WT and *Cib1*<sup>-/-</sup> hearts (Fig. 4d). The specificity of the all membrane fractions was verified by Western blotting for the sarcoplasmic reticulum Ca<sup>2+</sup> ATPase 2 (SERCA2), pan-cadherin and integrin  $\beta$ 1, while GAPDH was enriched in the cytosolic fraction. The specificity of the plasma membrane specific fraction was shown with the Na<sup>+</sup>/K<sup>+</sup> ATPase and the lack of SERCA2 (sarcoplasmic reticulum) and the lack of GAPDH (Fig 4c). While TAC stimulation enriched several proteins at the plasma membrane (Na<sup>+</sup>/K<sup>+</sup> ATPase) in both WT and *Cib1*<sup>-/-</sup> hearts, only the WT hearts showed calcineurin association with TAC at this site.

To further characterize this loss in CnB at the sarcolemma in the absence of CIB1, we cultured cardiac myocytes from adult WT and *Cib1*<sup>-/-</sup> mice and performed CnB immunostaining. CnB was localized at the sarcolemma in WT cardiomyocytes, but was displaced in myocytes from *Cib1*<sup>-/-</sup> mice (Fig. 4e). CnB could be retargeted to the membrane of *Cib1*<sup>-/-</sup> adult myocytes by AdCIB1 infection, but not with a mutant version of CIB1 (CIB1<sup>ΔN</sup>) that lacks the N-terminal myristoylation site (Fig. 4e). CIB1<sup>ΔN</sup> was also no longer able to associate with the plasma membrane in infected cultured cardiomyocytes (Fig. 4f). Collectively, these data suggest that CIB1 is necessary for anchoring calcineurin at the sarcolemma.

### CIB1 activates calcineurin/NFAT signaling

Given that CIB1 interacts with calcineurin and is responsible for its sarcolemmal localization, we further hypothesized that CIB1 might directly regulate calcineurin signaling. To measure the impact of CIB1 on calcineurin-NFAT activity, we infected neonatal cardiomyocytes with an NFAT-luciferase reporter adenovirus, with and without AdCIB1 (Fig. 5a). While AdCIB1 alone did not activate the NFAT-luciferase reporter versus Ad $\beta$ gal infection, AdCIB1 dramatically enhanced stimulus-induced NFAT activity through the pro-hypertrophic  $\alpha$ 1-adrenergic agonist PE (Fig. 5a). This synergistic increase in NFAT activity associated with AdCIB1 was blocked by overexpression of the calcineurin inhibitor Cain, indicating that the increase in NFAT activity is a direct effect of CIB1 on calcineurin, rather than NFAT. However, overexpression of CIB1<sup>ΔN</sup>, which cannot localize to the membrane, was not nearly as effective in augmenting PE-induced NFAT-luciferase reporter activity, suggesting that CIB1 enhances calcineurin-NFAT activity through a membrane localization-dependent mechanism (Fig. 5b). As a control, CIB1 did not directly induce CnA phosphatase activity in vitro using recombinant proteins (Fig. 5c), indirectly supporting the hypothesis that CIB1 augments calcineurin activity through membrane targeting.

To further investigate the mechanism whereby CIB1 regulates calcineurin and the hypertrophic response we examined NFAT activation in cultured cardiomyocytes. CIB1 siRNA transfection significantly reduced NFAT activation in PE-stimulated myocytes versus transfection of control siRNA (Fig. 5d,  $P < 0.05$ ). The effectiveness of the siRNA-mediated knockdown of CIB1 in this assay is shown in Supplemental Fig. 3c. We also crossed *Cib1*<sup>-/-</sup> mice with NFAT luciferase reporter transgenic mice and subjected them to 1 week of TAC. The data show that while WT mice displayed a significant elevation in NFAT-luciferase activity after TAC, mice lacking *Cib1* were unable to elicit an NFAT response with this reporter transgene (Fig. 5e,  $P < 0.05$ ). These data indicate that CIB1 is an important activator of calcineurin-NFAT signaling in hypertrophied cardiomyocytes.

CIB1 is similar in structure to CnB, both being small EF-hand-containing Ca<sup>2+</sup> binding proteins, suggesting the possibility that CIB1 might substitute for CnB in regulating CnA activity. However, Western blotting for CnB and CnA in *Ppp3r1* (CnB1)-deleted MEFs showed that CIB1 overexpression was unable to stabilize endogenous CnA protein levels in the absence of CnB protein, suggesting that CIB1 is not functionally equivalent to CnB (Fig. 5f). Calcineurin was also shown to associate with the L-type Ca<sup>2+</sup> channel in cardiac myocytes<sup>10</sup>, which resides in the sarcolemma where it might also be part of the CIB1 complex. Indeed, we observed that CIB1 interacted with the  $\alpha 1C$  subunit of the L-type Ca<sup>2+</sup> channel in TAC stimulated hearts, but not at rest (Fig. 5g). Mapping of this interaction showed that the region immediately N-terminal to the EF-hand domains of CIB1 (amino acids 82–108) are necessary for  $\alpha 1C$  protein interaction using a GST pull-down assay from cardiomyocyte protein extracts (Fig. 5h). These data raised the possibility that CIB1 might be part of another mechanism for recruiting calcineurin to the L-type Ca<sup>2+</sup> channel for activation. Indeed, the reduction in NFAT-luciferase activity due to CIB1 siRNA was not further reduced by verapamil (10  $\mu$ M, an L-type Ca<sup>2+</sup> channel inhibitor), and verapamil was equally potent in reducing PE-stimulated NFAT activity as CIB1 siRNA, collectively suggesting they might be part of the same activation mechanism (Fig. 5i).

### Characterization of CIB1 transgenic mice

Myocardial CIB1 is upregulated by 2-fold during pressure overload. Here we modeled this increase in CIB1 by generating tetracycline-inducible transgenic mice with cardiac-specific expression of this protein based on the  $\alpha$ MHC promoter<sup>22</sup> (Fig. 6a). This inducible system utilizes a driver transgene expressing the tetracycline activator protein (tTA) in the presence of the CIB1 responder transgene, so that double transgenic (DTG) mice in the absence of tetracycline or doxycycline (DOC) have protein expression (Fig. 6b). For all experiments DOX was removed at 1 month of age in DTG mice producing 2.5-fold overexpression of CIB1 in the heart in both line 26.6 and 27.5. However, if line 27.5 DTG mice were never treated with DOX during development, the overexpression level of CIB1 was 10-fold that of endogenous levels in 3 month-old mice (Fig. 6b). Neither 2.5- nor 10-fold overexpression of CIB1 affected cardiac function or hypertrophy at baseline (Supplemental Table).

Functionally, CIB1 overexpression from both lines (2.5-fold) significantly enhanced the cardiac hypertrophic response compared with control mice (non-transgenic mice and single  $\alpha$ MHC-tTA transgenic mice, Fig. 6c,  $P < 0.05$ ). In order to determine whether this enhanced

hypertrophic response was associated with increases in calcineurin-NFAT signaling, we also crossed CIB1 inducible transgenic mice to contain the NFAT-luciferase reporter transgene. The data show a significant increase in NFAT activity when CIB1 was overexpressed during TAC stimulation (Fig. 6d,  $P < 0.05$ ). Similarly, CIB1 overexpression in cultured cardiomyocytes by adenoviral gene transfer significantly enhanced PE-induced cardiomyocyte hypertrophy (Fig. 6e,  $P < 0.05$ ). CIB1 overexpression in transgenic hearts had no effect on other signaling pathways that were interrogated, such as MAPK, Akt/GSK3 $\beta$ , and NF $\kappa$ B (Supplemental Fig. 6).

We also crossed CIB1 inducible transgenic mice with mice containing the cardiac-specific activated calcineurin A transgene (CnA). CnA transgenic mice are known to have robust cardiac hypertrophy<sup>23</sup>. Here we observed that this hypertrophy is associated with increased myocardial expression of the CnB protein, which is the direct target of CIB1 (Fig. 6f). Interestingly, overexpression of CIB1 enhanced the hypertrophy response driven by the CnA transgene (Fig. 6g), indicating that calcineurin activation can be augmented by CIB1 in vivo. The reciprocal relationship was also investigated by crossing CIB1 inducible transgenic mice into the *Ppp3cb* (calcineurin A $\beta$  protein) null background. We previously demonstrated that *Ppp3cb*<sup>-/-</sup> mice are partially protected from pressure overload hypertrophy<sup>24</sup>. Interestingly, CIB1 overexpression did not lead to an augmentation of cardiac hypertrophy in the *Ppp3cb*<sup>-/-</sup> background compared to strain-matched backcrossed animals that were WT for *Ppp3cb*, suggesting that CIB1 is upstream of CnA (Fig. 6h). Together, these results suggest a model in which CIB1 is necessary to facilitate calcineurin activation, likely in association with the sarcolemma and possibly due to the presence of a specific Ca<sup>2+</sup> microdomain.

## DISCUSSION

Here we identified CIB1 as a novel regulator of pathological cardiac hypertrophy and calcineurin/NFAT signaling in cardiac myocytes. CIB1 shares substantial homology with CnB, calmodulin and neuronal calcium sensory (NCS) proteins like KChip, frequenin and neurocalcin. Based on structural criteria, CIB1 and the homologous proteins CIB2, 3 and 4, form a distinct subfamily of these small EF-hand domain proteins, suggesting unique functions<sup>14</sup>. CIB2 is highly expressed in skeletal muscle, but not in the heart, and is localized to the sarcolemma, myotendinous, and neuromuscular junctions<sup>25</sup>. Similarly, we observed CIB1 at the sarcolemma in both adult mouse and human heart, and this membrane localization was enhanced during hypertrophy, although some expression was observed more diffusely throughout the cytoplasm. It was previously shown that CIB1 localizes to the plasma-membrane in fibroblasts, human venous endothelial cells, and cultured platelets<sup>15</sup>. In HeLa cells, overexpressed CIB1 was detected in the nucleus, at the plasma-membrane, and in the endoplasmic reticulum but CIB1 mutants defective in myristoylation were displaced from the membrane and were found in a diffuse cytoplasmic and nuclear localization<sup>13,26</sup>.

Myocardial CIB1 expression is relatively high before birth and gradually becomes downregulated towards adulthood. However, CIB1 is re-induced in the adult heart during pathological hypertrophy, similar to other cardiac “fetal program” genes associated with hypertrophy, such as ANF, BNP, skeletal  $\alpha$ -actin and  $\beta$ MHC<sup>3,27</sup>. We demonstrate here that

upregulation of CIB1 is functionally important during pressure overload, as *Cib1*<sup>-/-</sup> mice have a significant loss in the hypertrophic response after 2 weeks of TAC, while overexpressing transgenic mice show augmented hypertrophy (P<0.05). Chronic exposure to increased hemodynamic load on the heart triggers adaptive and maladaptive signaling pathways in producing hypertrophy. While inhibition of the maladaptive pathways is a desirable goal of anti-hypertrophic therapies/strategies toward preventing heart failure, simultaneous inhibition of adaptive signaling pathways would be detrimental<sup>27</sup>. Examples for the latter include deletion of either *Melusin* or *Akt1*, which result in reduced cardiac hypertrophy, but also the development of heart failure in mice<sup>28,29</sup>. *Cib1* abrogation preserves cardiac function, capillary density, and diminishes myocardial fibrosis during chronic pressure overload, much like deletion of *Ppp3cb* (CnAβ)<sup>24</sup>, and is therefore a preferable target to inhibit maladaptive signaling. In support of this notion, *Cib1* deletion did not affect exercise-induced cardiac hypertrophy, which is associated with adaptive intracellular signaling.

The identification of CnB as a CIB1 interacting protein in the yeast two-hybrid screen naturally suggested a mechanism underlying the observed alterations in cardiac hypertrophy associated with CIB1 overexpression or abrogation. CnB is the exclusive and obligate binding partner of the CnA catalytic subunit, and neither protein is appreciably stable without expression of the other<sup>30</sup>. Calcineurin is a pro-hypertrophic signaling mediator that functions primarily through NFAT transcription factors in maladaptive programming of cardiac growth<sup>4,31,32</sup>. Overexpression of CIB1 facilitated calcineurin-NFAT activation, while downregulation of CIB1 impaired calcineurin-NFAT signaling in cardiac myocytes and hearts of transgenic mice.

Since CIB1 is localized at the sarcolemma, we hypothesized that it could target calcineurin to this region of the cell to allow sensing of Ca<sup>2+</sup> levels that might be different from total intracellular Ca<sup>2+</sup> levels involved in regulating myocyte contraction. Calcineurin association with the plasma-membrane was reported previously<sup>5,33</sup>. Calcineurin can also interact with the L-type Ca<sup>2+</sup> channel at the plasma membrane in the heart where it activates the channel to increase Ca<sup>2+</sup> influx<sup>10</sup>. Since calcineurin is activated by Ca<sup>2+</sup>, possibly from the L-type channel itself, a feed forward loop was proposed in activating a pool of calcineurin<sup>10</sup>. We demonstrate that CIB1 interacts with the L-type Ca<sup>2+</sup> channel and calcineurin, and that CIB1 enables its translocation to the sarcolemma. Indeed, CnB is unable to localize to the sarcolemma in *Cib1*<sup>-/-</sup> cardiomyocytes and a non-membrane targeting version of CIB1 was not nearly as effective in enhancing NFAT activation after stimulation as full-length CIB1, nor did it allow CnB to associate with the cell membrane. Moreover, in primary rat cardiomyocytes, in which the L-type Ca<sup>2+</sup> channel was inhibited (by verapamil), the effect of CIB1 downregulation on calcineurin/NFAT activation is abolished. Previous work also revealed the importance of calcineurin's membrane localization, for example, calcineurin can interact with phospholipids through CnB, which reportedly enhances its activation in vitro<sup>9,34</sup>. Furthermore, recent data suggest that the membrane anchoring and PDZ-domain containing protein PICK1 interacts with CnB and is necessary for calcineurin/NFAT activation<sup>35</sup>. Regardless of the entirety of the mechanism, CIB1 is clearly required for permitting activation of calcineurin during maladaptive cardiac hypertrophy, suggesting a



novel strategy for positively affecting hypertrophic heart disease through inhibition of CIB1 or its interaction with calcineurin.

## MATERIALS AND METHODS

### Animals and animal procedures

*Cib1* null mice have been reported previously<sup>20,21</sup>. The tetracycline responsive binary  $\alpha$ MHC transgene system was used to overexpress CIB1 in myocytes of the heart<sup>22</sup>. Doxycycline was administered in the food using a diet formulated by Purina (625 mg/kg food). Double transgenic mice were crossed with mice expressing the CnA transgene<sup>23</sup>, with NFAT-luciferase reporter transgenic mice and with mice lacking *Ppp3cb*<sup>24,36</sup>. TAC was performed as previously described<sup>24,36</sup>. Swimming was conducted for 3 weeks as described previously<sup>36</sup>. For echocardiography, mice were anesthetized with 2% isoflurane and scanning was performed using a Hewlett Packard Sonos 5500 instrument with a 15-MHz transducer as described before<sup>24</sup>. Animal experiments were approved by the Animal Care and Use Committee of Cincinnati Children's Hospital Medical Center.

### Western Blotting, RT-PCR and Northern blotting

Western blot analysis was performed using the following antibodies: phospho-Akt (Serine 473), Akt, phospho-GSK3 $\beta$  (Serine 9), GSK3 $\beta$ , phospho-ERK1/2, ERK 1/2, phospho-JNK, JNK, phospho-p38, p38, Myc-Tag (Cell Signaling Technology), CIB1 (Zymed Laboratories Inc.), Pan-CnA, atrial natriuretic factor (Chemicon International), CnB (Upstate), pan-cadherin and Na<sup>+</sup>/K<sup>+</sup> ATPase (Abcam),  $\beta$ 1-intergrin, GST, I $\kappa$ B- $\alpha$ , SERCA2 (Santa Cruz Biotechnology Inc.),  $\alpha$ 1C subunit of the L-type Ca<sup>2+</sup> channel (Alomone labs) and GAPDH (Fitzgerald Industries Intl). RNA from cells or tissue was isolated using TRIZOL reagent (Gibco) and RT-PCR and Northern Blot analyses were conducted as previously described<sup>36,37</sup>.

### Histological Analysis

Sections for Masson's Trichrome staining were generated from paraffin embedded hearts. Fibrosis was quantified through image analysis with MetaMorph 6.1 software (Universal Imaging Corp.) as described previously in detail<sup>38</sup>. Frozen sections were also used to visualize myocardial capillaries with isolectin B4 (Vector) and cardiomyocyte cell membranes by staining with TRITC-conjugated wheat-germ agglutinin (Sigma-Aldrich). Immunostaining for CIB1 and CnB was performed on cryosections of human and mouse myocardium, or cultured cells. After fixation, the primary antibody for CnB (Upstate) or CIB1 (Santa Cruz Biotechnologies) was incubated overnight before it was visualized with ALEXA 488 or ALEXA 568 linked secondary antibodies (Invitrogen). As a negative control, the primary antibody incubation was omitted in the procedure. The human heart samples used in this study were described previously<sup>39</sup>. Between 10 and 20 mg of frozen heart tissue was used to analyze collagen content through biochemical assessment of hydroxyproline content, as described in detail previously<sup>38</sup>.

### Yeast two-hybrid analysis

The Matchmaker Gal4 two-hybrid system 3 (Clontech) was used for screening according to the manufacturer's instructions, and as described before<sup>40</sup>. The bait construct consisted of full-length mouse CIB1 cloned in frame into the EcoRI and BamHI sites of pGBKT7 using PCR generated linkers. This bait was used to screen a mouse adult cardiac cDNA library constructed into the EcoRI site of pGAD10 (custom made, Clontech). The initial screen was carried out on medium stringency complete medium lacking tryptophan, leucine and histidine, plus 5 mM 3-amino-1,2,4-triazole. Interactions were confirmed by cotransformation of pGBKT7-CIB1 or pGBKT7-empty vector with either pGAD10-empty, pGAD10-CnB<sub>short</sub>, or pGAD10-CnB<sub>long</sub> in AH109 yeast cells and subsequent plating of the resulting clones on medium stringency agar plates in the presence of X-gal. Cotransformation of pGBKT7-CnB<sub>short</sub> and pGAD-CnA served as a positive control.

### GST Pull-Down Assays

To generate GST fusion proteins, CIB1 cDNA sequences were amplified by PCR and cloned into pGEX-4T-1 (Amersham Pharmacia Biotech). The fusion proteins were expressed in *E. coli* BL21 cells (Invitrogen) and precipitated with glutathione-sepharose beads (GE Healthcare). Binding assays with the different sepharose bound GST fusion proteins were performed with in vitro synthesized [<sup>35</sup>S]methionine-labeled CnB<sub>short</sub> or with protein lysates from primary neonatal cardiomyocytes.

### Isolation of plasma and total membrane proteins

For extraction of plasma-membrane and total membrane proteins, frozen whole hearts were first disintegrated using a mortar and pestle and then subjected to homogenization with a Dounce homogenizer in homogenizing buffer (BioVision kit) and the manufacturer's protocol was followed in subsequent steps as previously described<sup>41,42</sup>.

### Cell Culture

Primary neonatal rat cardiomyocytes were prepared from hearts of 1–2-day old Sprague-Dawley rat pups as previously described<sup>40</sup>. Adult mouse cardiac myocytes were isolated following a modified protocol as previously described<sup>43</sup>. Mouse embryonic fibroblasts were isolated from WT or *Ppp3r1* (CnB1) loxP-targeted (flox/flox) mice as previously described<sup>44,45</sup>.

### Adenoviral constructs and siRNA

Adβgal, AdCnB (short), AdCain and AdNFAT-luc were previously described<sup>40</sup>. To generate recombinant adenoviruses, the mouse, human, and truncated human CIB1 cDNAs were subcloned into the pShuttle-CMV vector using the AdEasy XL Adenoviral Vector system as previously described<sup>40</sup> (Stratagene). The human full-length and N-terminal deletion of CIB1 contained a C-terminal myc tag. Neonatal cardiac myocytes were infected with adenoviruses as described previously at a multiplicity of infection of 25–50<sup>40</sup>. Adult mouse cardiac myocytes were transduced at a multiplicity of infection of 200–400 for 1 hour in myocyte culture media before the cells were switched to fresh media<sup>43</sup>. To downregulate CIB1 in rat neonatal cardiomyocytes, we transfected cells with anti-CIB1 siRNA (Ambion,

sense strand: 5'-GGAGCGAAUCUGCAUGGUUCTT-3') or a negative-control siRNA (Ambion) at a final concentration of 100 nM using Lipofectamine 2000 (Invitrogen).

### Immunoprecipitation

Neonatal cardiomyocytes were infected with specific adenoviruses for 48 hrs. For immunoprecipitation with the anti-CnB, anti-CnA, anti-CIB1 antibodies (4 µg), cardiomyocytes or whole hearts were harvested in lysis buffer containing 20 mM Hepes, 75 mM NaCl, and 0.05% NP-40. The immuno-complexes were captured with Protein A/G PLUS Agarose beads (Santa Cruz), and after extensive washing the proteins were resolved with SDS-PAGE electrophoresis and subjected to Western blotting.

### Luciferase Assays

AdNFAT-luc was used to infect neonatal cardiomyocytes that were either additionally infected with other recombinant adenoviruses or were transfected with either control or CIB1 siRNA for 24 hrs before PE (10 µM, Sigma-Aldrich) or verapamil (10 µM, Sigma-Aldrich) was added for 24 or 48 hrs. The cells were then harvested to determine luciferase activity as previously described<sup>40</sup>. Essentially 100% of the myocytes are infected with the luciferase reporter, so samples were only normalized to total protein and not with another co-infected reporter, although similar results were obtained when a co-transfection reporter control was used for normalization.

### Calcineurin Activity Assay

Recombinant calcineurin activity was measured as the dephosphorylation rate of a synthetic phosphopeptide substrate (RII peptide) using an assay kit (Biomol) according to the manufacturer's instructions.

### Statistics

All values are presented as mean ± SEM. Differences between 2 groups were analyzed by unpaired Student's t test. Differences between 3 or more groups were analyzed by 1-way ANOVA followed by Student-Newman-Keuls post-hoc test. A 2-tailed P value of less than 0.05 was considered to indicate statistical significance.

### Supplementary Material

Refer to Web version on PubMed Central for supplementary material.

### Acknowledgments

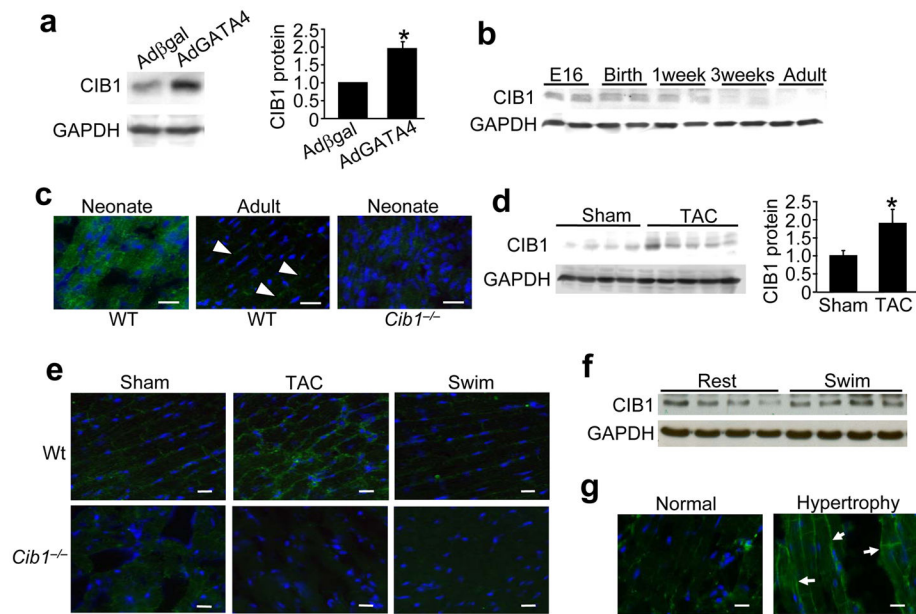
This work was supported by grants from the National Institutes of Health (J.D.M., L.V.P.), the Howard Hughes Medical Institute (J.D.M.) and by the Fondation Leducq (J.D.M and H.D.). J. H. was supported in part by a grant from the Deutsche Forschungsgemeinschaft (DFG), Bonn, Germany (HE 3658/1-1) and the Cluster of Excellence Rebirth (also DFG). M.B. was supported by NIH training grant 5 T32 HL07382 (principal investigator Arnold Schwartz).

## References

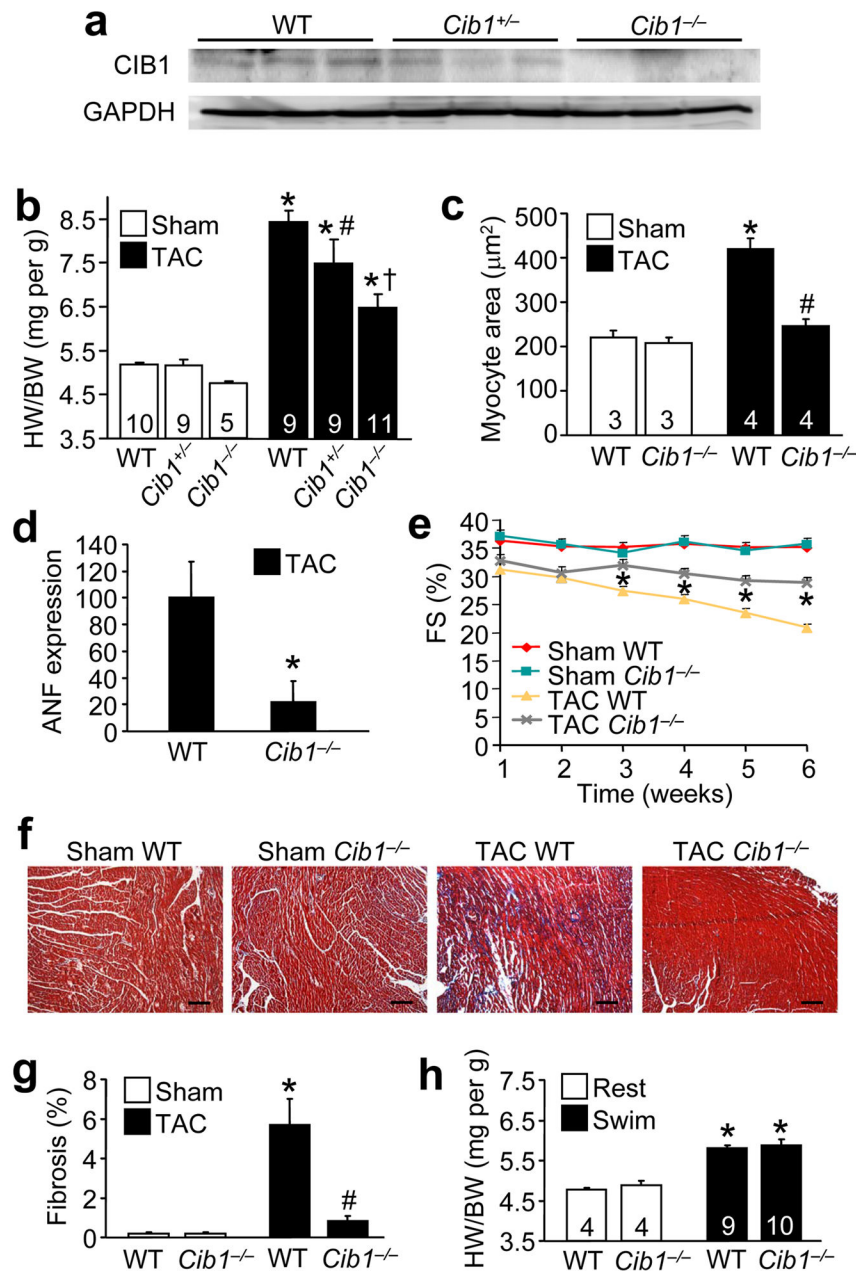
1. Rosamond W, et al. Heart disease and stroke statistics--2008 update: a report from the American Heart Association Statistics Committee and Stroke Statistics Subcommittee. *Circulation*. 2008; 117:e25–146. [PubMed: 18086926]
2. Levy D, Larson MG, Vasani RS, Kannel WB, Ho KK. The progression from hypertension to congestive heart failure. *Jama*. 1996; 275:1557–1562. [PubMed: 8622246]
3. Heineke J, Molkentin JD. Regulation of cardiac hypertrophy by intracellular signalling pathways. *Nat Rev Mol Cell Biol*. 2006; 7:589–600. [PubMed: 16936699]
4. Bueno OF, van Rooij E, Molkentin JD, Doevendans PA, De Windt LJ. Calcineurin and hypertrophic heart disease: novel insights and remaining questions. *Cardiovasc Res*. 2002; 53:806–821. [PubMed: 11922891]
5. Buch MH, et al. The sarcolemmal calcium pump inhibits the calcineurin/nuclear factor of activated T-cell pathway via interaction with the calcineurin A catalytic subunit. *J Biol Chem*. 2005; 280:29479–29487. [PubMed: 15955804]
6. Frey N, Richardson JA, Olson EN. Calsarcins, a novel family of sarcomeric calcineurin-binding proteins. *Proc Natl Acad Sci USA*. 2000; 97:14632–14637. [PubMed: 11114196]
7. Heineke J, et al. Attenuation of cardiac remodeling after myocardial infarction by muscle LIM protein-calcineurin signaling at the sarcomeric Z-disc. *Proc Natl Acad Sci USA*. 2005; 102:1655–1660. [PubMed: 15665106]
8. Jeong D, et al. PICOT attenuates cardiac hypertrophy by disrupting calcineurin-NFAT signaling. *Circ Res*. 2008; 102:711–719. [PubMed: 18258855]
9. Politino M, King MM. Calcineurin-phospholipid interactions. Identification of the phospholipid-binding subunit and analyses of a two-stage binding process. *J Biol Chem*. 1990; 265:7619–7622. [PubMed: 2159005]
10. Tandan S, et al. Physical and functional interaction between calcineurin and the cardiac L-type Ca<sup>2+</sup> channel. *Circ Res*. 2009; 105:51–60. [PubMed: 19478199]
11. Saito T, et al. Structure, expression profile, and chromosomal location of a mouse gene homologous to human DNA-PKcs interacting protein (KIP) gene. *Mamm Genome*. 1999; 10:315–317. [PubMed: 10051332]
12. Shock DD, et al. Calcium-dependent properties of CIB binding to the integrin alphaIIb cytoplasmic domain and translocation to the platelet cytoskeleton. *Biochem J*. 1999; 342(Pt 3):729–735. [PubMed: 10477286]
13. Stabler SM, Ostrowski LL, Janicki SM, Monteiro MJ. A myristoylated calcium-binding protein that preferentially interacts with the Alzheimer's disease presenilin 2 protein. *J Cell Biol*. 1999; 145:1277–1292. [PubMed: 10366599]
14. Gentry HR, et al. Structural and biochemical characterization of CIB1 delineates a new family of EF-hand-containing proteins. *J Biol Chem*. 2005; 280:8407–8415. [PubMed: 15574431]
15. Naik MU, Naik UP. Calcium-and integrin-binding protein regulates focal adhesion kinase activity during platelet spreading on immobilized fibrinogen. *Blood*. 2003; 102:3629–3636. [PubMed: 12881299]
16. Haataja L, Kaartinen V, Groffen J, Heisterkamp N. The small GTPase Rac3 interacts with the integrin-binding protein CIB and promotes integrin alpha(IIb)beta(3)-mediated adhesion and spreading. *J Biol Chem*. 2002; 277:8321–8328. [PubMed: 11756406]
17. Leisner TM, Liu M, Jaffer ZM, Chernoff J, Parise LV. Essential role of CIB1 in regulating PAK1 activation and cell migration. *J Cell Biol*. 2005; 170:465–476. [PubMed: 16061695]
18. Naik UP, Patel PM, Parise LV. Identification of a novel calcium-binding protein that interacts with the integrin alphaIIb cytoplasmic domain. *J Biol Chem*. 1997; 272:4651–4654. [PubMed: 9030514]
19. Jarman KE, Moretti PA, Zebol JR, Pitson SM. Translocation of sphingosine kinase 1 to the plasma membrane is mediated by calcium and integrin binding protein 1. *J Biol Chem*. 2009 Oct 23. [Epub ahead of print].
20. Yuan W, et al. CIB1 is essential for mouse spermatogenesis. *Mol Cell Biol*. 2006; 26:8507–8514. [PubMed: 16982698]

21. Zayed MA, et al. CIB1 regulates endothelial cells and ischemia-induced pathological and adaptive angiogenesis. *Circ Res.* 2007; 101:1185–1193. [PubMed: 17975111]
22. Sanbe A, et al. Reengineering inducible cardiac-specific transgenesis with an attenuated myosin heavy chain promoter. *Circ Res.* 2003; 92:609–616. [PubMed: 12623879]
23. Molkentin JD, et al. A calcineurin-dependent transcriptional pathway for cardiac hypertrophy. *Cell.* 1998; 93:215–228. [PubMed: 9568714]
24. Bueno OF, et al. Impaired cardiac hypertrophic response in Calcineurin Abeta -deficient mice. *Proc Natl Acad Sci USA.* 2002; 99:4586–4591. [PubMed: 11904392]
25. Hager M, et al. Cib2 Binds Integrin {alpha}7B{beta}1D and Is Reduced in Laminin {alpha}2 Chain-deficient Muscular Dystrophy. *J Biol Chem.* 2008; 283:24760–24769. [PubMed: 18611855]
26. Zhu J, Stabler SM, Ames JB, Baskakov I, Monteiro MJ. Calcium binding sequences in calmyrin regulates interaction with presenilin-2. *Exp Cell Res.* 2004; 300:440–454. [PubMed: 15475008]
27. Frey N, Katus HA, Olson EN, Hill JA. Hypertrophy of the heart: a new therapeutic target? *Circulation.* 2004; 109:1580–1589. [PubMed: 15066961]
28. DeBosch B, et al. Akt1 is required for physiological cardiac growth. *Circulation.* 2006; 113:2097–2104. [PubMed: 16636172]
29. Brancaccio M, et al. Melusin, a muscle-specific integrin beta1-interacting protein, is required to prevent cardiac failure in response to chronic pressure overload. *Nat Med.* 2003; 9:68–75. [PubMed: 12496958]
30. Parsons SA, et al. Genetic loss of calcineurin blocks mechanical overload-induced skeletal muscle fiber type switching but not hypertrophy. *J Biol Chem.* 2004; 279:26192–26200. [PubMed: 15082723]
31. Bourajaj M, et al. NFATc2 is a necessary mediator of calcineurin-dependent cardiac hypertrophy and heart failure. *J Biol Chem.* 2008; 283:22295–22303. [PubMed: 18477567]
32. Wilkins BJ, et al. Targeted disruption of NFATc3, but not NFATc4, reveals an intrinsic defect in calcineurin-mediated cardiac hypertrophic growth. *Mol Cell Biol.* 2002; 22:7603–7613. [PubMed: 12370307]
33. Li W, Handschumacher RE. Identification of two calcineurin B-binding proteins: tubulin and heat shock protein 60. *Biochim Biophys Acta.* 2002; 1599:72–81. [PubMed: 12479407]
34. Politino M, King MM. Calcium- and calmodulin-sensitive interactions of calcineurin with phospholipids. *J Biol Chem.* 1987; 262:10109–10113. [PubMed: 3611055]
35. Iida T, Egusa H, Saeki M, Yatani H, Kamisaki Y. PICK1 binds to calcineurin B and modulates the NFAT activity in PC12 cells. *Biochem Biophys Res Commun.* 2008
36. Wilkins BJ, et al. Calcineurin/NFAT coupling participates in pathological, but not physiological, cardiac hypertrophy. *Circ Res.* 2004; 94:110–118. [PubMed: 14656927]
37. Heineke J, et al. Downregulation of cytoskeletal muscle LIM protein by nitric oxide: impact on cardiac myocyte hypertrophy. *Circulation.* 2003; 107:1424–1432. [PubMed: 12642365]
38. Parsons SA, Millay DP, Sargent MA, McNally EM, Molkentin JD. Age-dependent effect of myostatin blockade on disease severity in a murine model of limb-girdle muscular dystrophy. *Am J Pathol.* 2006; 168:1975–1985. [PubMed: 16723712]
39. Haq S, et al. Differential activation of signal transduction pathways in human hearts with hypertrophy versus advanced heart failure. *Circulation.* 2001; 103:670–677. [PubMed: 11156878]
40. Liu Q, Wilkins BJ, Lee YJ, Ichijo H, Molkentin JD. Direct interaction and reciprocal regulation between ASK1 and calcineurin-NFAT control cardiomyocyte death and growth. *Mol Cell Biol.* 2006; 26:3785–3797. [PubMed: 16648474]
41. Vila-Carriles WH, Zhou ZH, Buben JK, Fuller CM, Benos DJ. Participation of the chaperone Hsc70 in the trafficking and functional expression of ASIC2 in glioma cells. *J Biol Chem.* 2007; 282:34381–34391. [PubMed: 17878160]
42. Jernigan NL, et al. Dietary salt enhances benzamil-sensitive component of myogenic constriction in mesenteric arteries. *Am J Physiol Heart Circ Physiol.* 2008; 294:H409–420. [PubMed: 18024548]

43. Kabaeva Z, Zhao M, Michele DE. Blebbistatin extends culture life of adult mouse cardiac myocytes and allows efficient and stable transgene expression. *Am J Physiol Heart Circ Physiol*. 2008; 294:H1667–1674. [PubMed: 18296569]
44. Baines CP, Kaiser RA, Sheiko T, Craigen WJ, Molkentin JD. Voltage-dependent anion channels are dispensable for mitochondrial-dependent cell death. *Nat Cell Biol*. 2007; 9:550–555. [PubMed: 17417626]
45. Neilson JR, Winslow MM, Hur EM, Crabtree GR. Calcineurin B1 is essential for positive but not negative selection during thymocyte development. *Immunity*. 2004; 20:255–266. [PubMed: 15030770]

**Figure 1.**

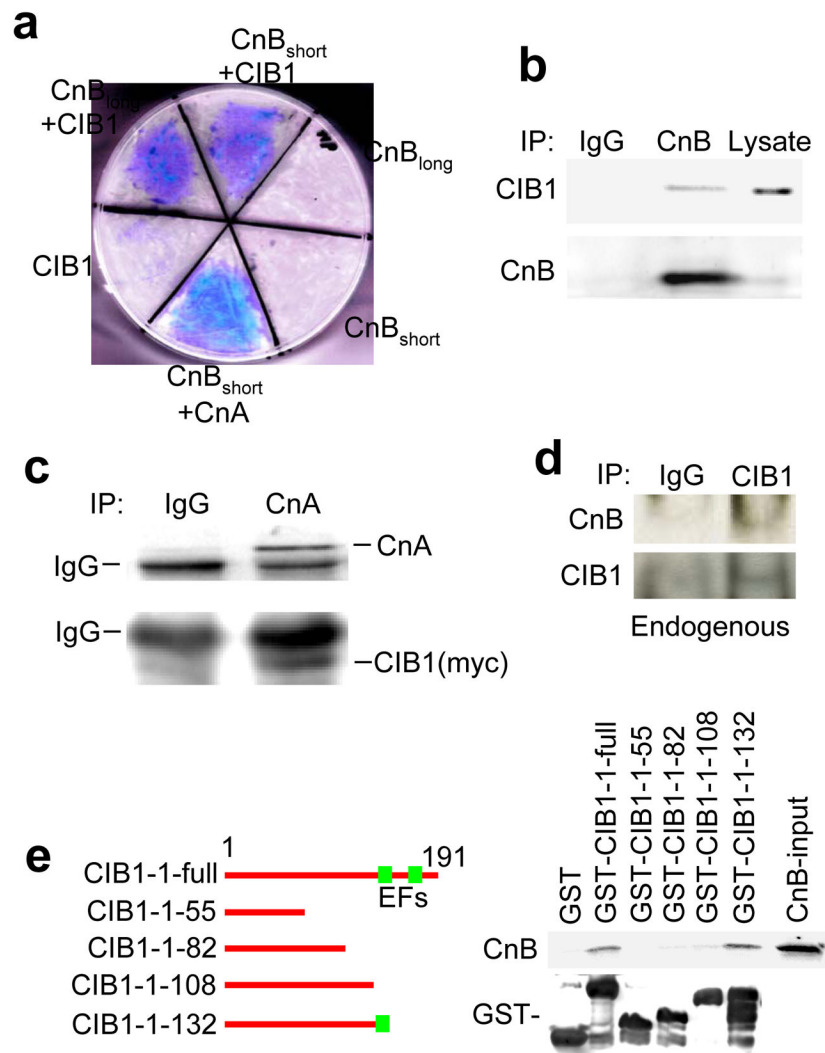
CIB1 is expressed in mouse and human heart. **(a)** Representative immunoblot for CIB1 and GAPDH (loading control) from rat neonatal cardiomyocytes infected with either Adβgal or AdGATA4. The quantification of these results is shown to the right, \* $p < 0.05$  vs. Adβgal,  $n = 3$  for each condition. **(b)** Representative immunoblot for CIB1 and GAPDH of whole cell lysates from mouse hearts at E16, birth, 1 and 3 weeks of age and adulthood. **(c)** Immunohistochemistry of frozen mouse heart sections stained for CIB1 (green) from WT and *Cib1*<sup>-/-</sup> hearts in neonates or adults. Nuclei are in blue. Representative images are shown. Scale bars: 20 μm. **(d)** Representative immunoblot and quantitation (right) for CIB1 and GAPDH from cardiac extracts of adult mice 2 weeks after sham or TAC surgery ( $n = 4-5$  mice per group). \* $p < 0.05$  vs. sham **(e)** Immunohistochemistry for CIB1 (green) in frozen mouse heart sections from WT or *Cib1*<sup>-/-</sup> mice after sham or TAC surgery or swimming exercise. Nuclei are in blue. Scale bars: 20 μm **(f)** Western blotting for CIB1 and GAPDH from mice at rest or after swimming exercise. **(g)** Immunohistochemistry of frozen human hearts sections for CIB1 (green), nuclei are shown in blue. Arrowheads show enriched localization at the sarcolemma in hypertrophied hearts. Scale bars: 20 μm.

**Figure 2.**

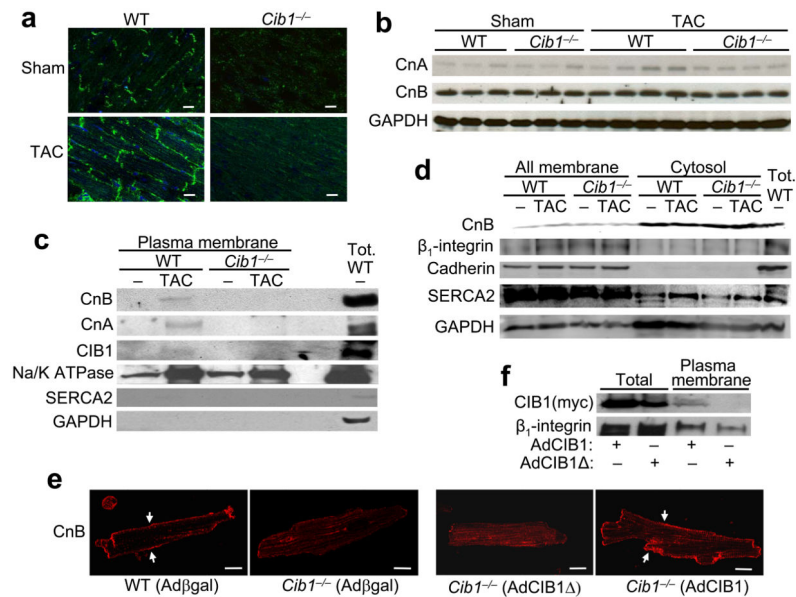
CIB1 is necessary for pathological but not physiological hypertrophy and contributes to cardiac dysfunction during pressure overload. (a) Western blotting for CIB1 in the heart of WT, *Cib1*<sup>+/-</sup> and *Cib1*<sup>-/-</sup> mice. GAPDH is a loading control. (b) Heart weight to body weight ratios (HW/BW) from wildtype (WT), heterozygous or homozygous *Cib1* gene-targeted mice 2 weeks after sham or TAC surgery. The number of mice per group is indicated within the bar. \*p<0.01 vs. control sham, #p<0.05 vs. WT TAC and *Cib1*<sup>-/-</sup> TAC, †p<0.001 vs. WT TAC. (c) Myocyte cross-sectional area in WT and *Cib1*<sup>-/-</sup> mice 2 weeks after sham or TAC surgery. \*p<0.001 vs. sham, #p<0.001 vs. WT TAC. (d) ANF levels from the indicated hearts after TAC. No expression was observed in sham-operated hearts.



\* $p < 0.05$  vs. WT TAC. **(e)** Fractional shortening (FS in %) determined by echocardiography in WT and *Cib1*<sup>-/-</sup> mice after sham or TAC surgery. \* $p < 0.01$  vs. WT sham and *Cib1*<sup>-/-</sup> TAC. N= 6–7 animals per sham group and N=15–18 animals per TAC group. **(f)** Representative images of Masson’s trichrome-stained paraffin-embedded heart sections from WT and *Cib1*<sup>-/-</sup> mice. Scale bars: 100  $\mu\text{m}$ . **(g)** Myocardial fibrosis as determined by MetaMorph software. N=3 per sham group, N=4 per TAC group, \* $p < 0.01$  vs. WT sham, # $p < 0.01$  vs. WT TAC. **(h)** HW/BW ratio of WT or *Cib1*<sup>-/-</sup> mice after 3 weeks of rest or swimming exercise. \* $p < 0.001$  vs. WT rest.

**Figure 3.**

CIB1 interacts with CnB. **(a)**  $\beta$ -galactosidase (blue) and growth assessment for protein-protein interaction by yeast two-hybrid analysis. The areas with blue staining represent proteins that are interacting in the assay. **(b)** Immunoblot for CIB1 (c-myc tag) or CnB after immunoprecipitation (IP) from AdCnB and AdCIB1-myc infected neonatal cardiomyocytes. CnB antibody or control IgG was used for the IP. **(c)** Immunoblot for CnA or CIB1 after IP from AdCnA and AdCIB1-myc infected neonatal cardiomyocytes. CnA antibody or control IgG was used for the IP. **(d)** Immunoblot for endogenous CnB or CIB1 after IP from WT mouse hearts. CIB1 antibody or control IgG was used for the IP. **(e)** GST pull-down assay showing a schematic of the different GST – CIB1 fusion constructs (left). The functional EF-hand domains are marked in green. The right panel shows an SDS PAGE of [<sup>35</sup>S]methionine-labeled CnB subject to pull-down with the indicated GST-CIB1 fusion constructs. An immunoblot shows the integrity of the GST fusion proteins.

**Figure 4.**

CIB1 expression is necessary for sarcolemmal localization of CnB. **(a)**

Immunohistochemistry of frozen mouse heart sections from WT and *Cib1*<sup>-/-</sup> mice subject to TAC or sham and stained for CnB (green). Nuclei are in blue. Scale bars: 20 μm. **(b)** Control immunoblots for CnA, CnB and GAPDH from mouse hearts of the indicated groups. **(c,d)** Representative immunoblots of specific subcellular protein fractions from WT and *Cib1*<sup>-/-</sup> hearts after sham or TAC surgery for the indicated proteins. **(e)** Adult cardiac myocytes from WT and *Cib1*<sup>-/-</sup> mice infected with Adβgal, AdCIB1 or AdCIB1Δ stained for CnB (red). Arrowheads show sarcolemmal localization of CnB. Scale bars: 20 μm. **(f)** Western blot for CIB1 and β<sub>1</sub>-integrin from the indicated protein extracts generated from cultured cardiomyocytes infected with either of the 2 shown adenoviruses.

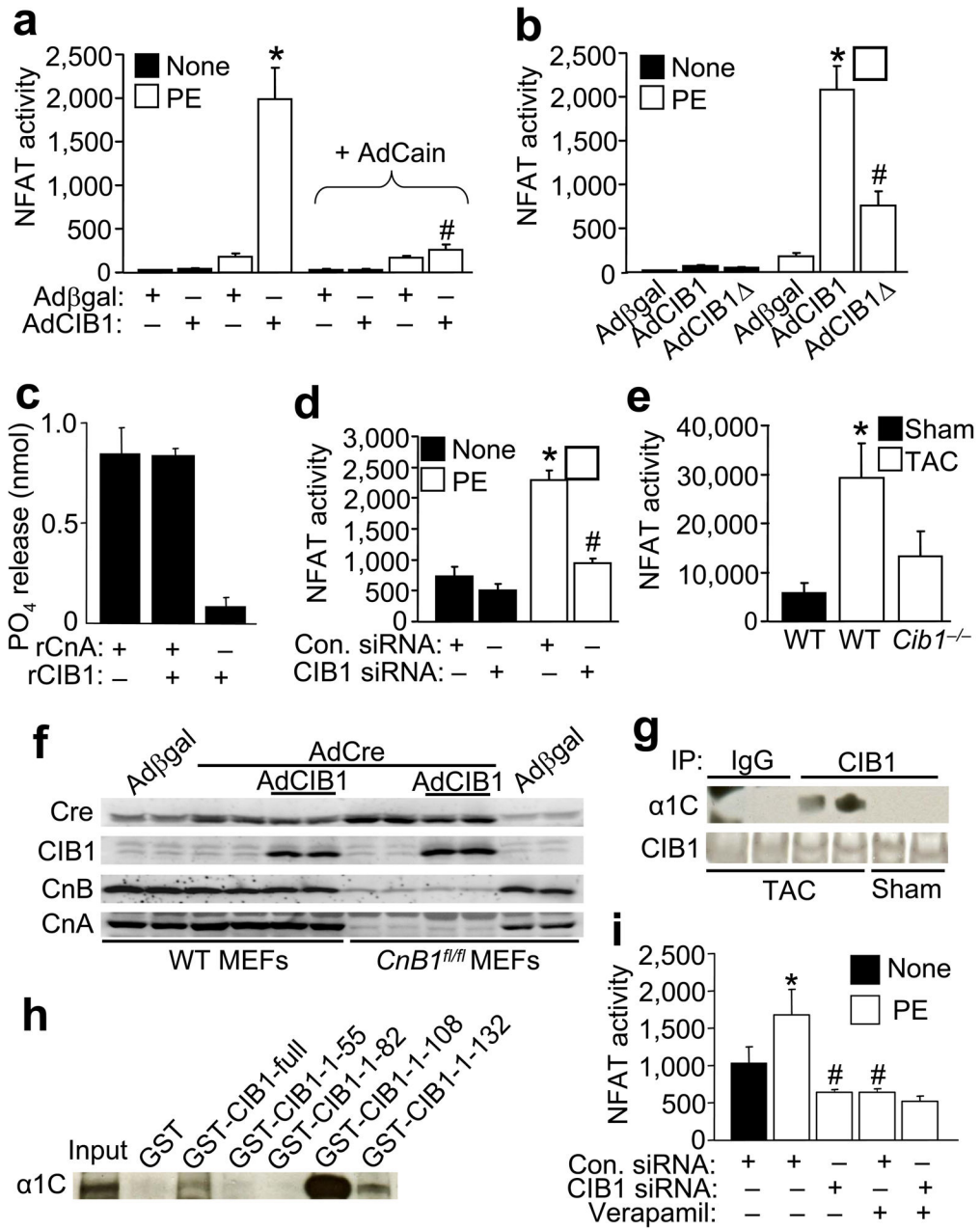


**Figure 5.** CIB1 facilitates calcineurin/NFAT activation. **(a)** Neonatal rat cardiac myocytes were infected with AdNFAT-luc and Adβgal, AdCIB1 or AdCain and stimulated with PE (10 μM) for 48 hrs as indicated. NFAT-dependent luciferase activity was measured and normalized to total protein content. N=6–15 per condition. \*p<0.001 vs. Adβgal and Adβgal + PE, #p<0.001 vs. AdCIB1 + PE. **(b)** Neonatal rat cardiac myocytes were infected with AdNFAT-luc and Adβgal, AdCIB1 or AdCIB1Δ and stimulated with PE for 48 hrs as indicated. N=5–15 per condition, \*p<0.001 vs. Adβgal and Adβgal + PE, #p<0.001 vs. AdCIB1 + PE. **(c)** Calcineurin phosphatase assay over 30 minutes against the phosphorylated RII peptide with recombinant calcineurin holoenzyme (2.5 μg = 20 units)

and CIB1 (5  $\mu$ g). **(d)** Neonatal rat cardiac myocytes were infected with AdNFAT-luc and transfected with control or CIB1 siRNA, then stimulated with PE for 24 hrs as indicated. N=6 per condition, \*p<0.001 vs. control siRNA, #p<0.001 vs. control siRNA + PE. **(e)** NFAT luciferase activity (normalized to total protein content) measured from NFAT-luc reporter transgenic mice WT or null (-/-) for *Cib1* after sham and TAC surgery as indicated. N=3–6 mice per condition, \*p<0.05 vs. WT sham. **(f)** Immunoblot for the indicated proteins from WT or *Ppp3r1<sup>fl/fl</sup>* mouse embryonic fibroblasts (MEFs) infected with Ad $\beta$ gal control or AdCre to delete CnB1 protein if appropriate. **(g)** Immunoblot for the  $\alpha$ 1C subunit of the L-type  $\text{Ca}^{2+}$  channel and CIB1 after IP from CIB1 overexpressing mouse hearts 2 weeks after TAC or sham operation. CIB1 antibody or control IgG was used for the IP. **(h)** Immunoblot against the  $\alpha$ 1C subunit of the L-type  $\text{Ca}^{2+}$  channel after a pull-down assay from neonatal cardiomyocyte lysate incubated with the indicated GST-CIB1 fusion constructs. **(i)** Neonatal rat cardiac myocytes were transfected with control or CIB1 siRNA and infected with AdNFAT-luc, then stimulated with PE and verapamil (10 $\mu$ M) for 24 hours as indicated. N=4–6 per condition, \*p<0.05 vs. control siRNA, #p<0.001 vs. control siRNA + PE.

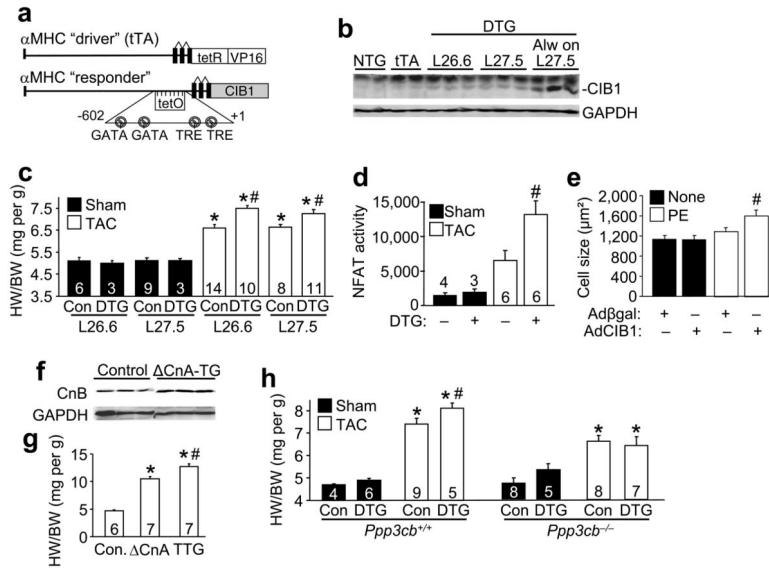


**Figure 6.** Myocardial CIB1 overexpression enhances hypertrophy and calcineurin/NFAT signaling during pressure overload. **(a)** Schematic representation of the binary transgenic constructs that drive inducible CIB1 expression in the heart. **(b)** Representative immunoblot for CIB1 and GAPDH (control) from whole cell lysates from hearts of 3 month-old non-transgenic (NTG), single αMHC-tTA (tTA), or αMHC<sub>TET</sub>-CIB1 × αMHC-tTA double transgenic (DTG) of line (L) 26.6 and 27.5 taken off DOX at 4 weeks of age, or DTG mice from line 27.5 that were never placed on DOX (Always on). **(c)** HW/BW 2 weeks after sham or TAC surgery from control (Con) and DTG mice of lines 26.6 and 27.5. The number of mice per group is indicated within the bar. \*p<0.001 vs. control sham from the same line, #p<0.05 vs. control TAC from the same line. **(d)** NFAT luciferase activity measured 1 week after sham or TAC surgery in control or DTG mice also harboring the NFAT-luciferase reporter transgene. The number of mice per group is indicated within or above the bar. #p<0.01 vs. control sham and control TAC. **(e)** Neonatal rat cardiomyocyte average cell size after PE stimulation for 24 hrs and prior infection with Adβgal (control) or AdCIB1. #p<0.01 vs. Adβgal + PE. **(f)** Representative immunoblot for CnB and GAPDH from whole cell protein lysates from WT control mice and αMHC- CnA-TG mice. **(g)** HW/BW from control mice, αMHC- CnA-TG mice and αMHC- CnA-TG × αMHC<sub>TET</sub>-CIB1 × αMHC-tTA triple transgenic (TTG) mice always off DOX. \*p<0.001 vs. control, #p<0.001 vs. αMHC- CnA-TG mice. **(h)** HW/BW of control and line 27.5 DTG mice (always off DOX) 2 weeks after sham or TAC surgery in WT (left panel) or in the *Ppp3cb*<sup>-/-</sup> (CnAβ) background (right panel). \*p<0.001 vs. control sham, #p<0.05 vs. control TAC.